Snow Microstructure Measurements Using Stereology

Jeff Dozier and Robert E. Davis
Department of Geography, University of California
Santa Barbara, CA 93106, U.S.A.

Ron Perla
National Hydrology Research Institute
Box 313, Canmore, Alberta TOL 0M0

1. Introduction

Snow is a network of ice grains interconnected in a complex structure. Liquid water may also be present, in an intricate configuration. The characteristics of this porous medium govern the response of snow to electromagnetic and mechanical energy and control the movement of heat, liquid water, and water vapor.

Stereology is a branch of mathematics relating three-dimensional parameters defining structure to two-dimensional measurements obtainable on sections of the structure [Weibel, 1979]. A section of the structure represents a planar sample of profiles of the objects of interest. The stereologic relations described here are simple. Although they are based on geometric probability and have been derived by complex mathematical reasoning, we present only the final relations and their necessary assumptions. Complete derivations and discussion can be found in Underwood [1970] and Weibel [1979, 1980].

Some properties of a snow sample can be calculated from a single random section image. Others require three-dimensional topological information, which can only be obtained from serial sections. For some properties detection of anisotropy is crucial, and it is essential to test planes parallel and perpendicular to the macrostratigraphy as observed in the field.

One method previously used to analyze the structure of the air and ice phases is to prepare thin sections, usually less than half a grain diameter in thickness, cut from specially prepared snow samples [Keeler, 1969; Good, 1982]. Preparing a thin section generally consists of cutting a plane in the sample, attaching the sample to a glass slide, and cutting a second plane to obtain the desired thickness. Thin sections using opaque pore fillers or other treatments create a two-dimensional profile

Presented at Workshop on Snow Property Measurement, Chateau Lake Louise, April 1-3, 1985.

or section image from which some of the properties of the three-dimensional structure can be calculated. The advantage of thin sections is that the bonds between individual grains can be identified and measured.

If structural properties other than bonding are required, the information may be obtainable from a plane section of a snow sample. Cutting a prepared snow sample with a single plane is less time-consuming and requires less care, provides the same measurements, and allows serial sectioning if topological information is required. Structural measurements of the ice phase in snow have been made from section images using manual analysis [Kry, 1975; Gubler, 1978] and computer-aided analysis [Vallese and Kong, 1981; Good, 1982; Perla, in press].

2. Sample Collection and Preparation

Samples are usually obtained from a snow pit at the same time conventional snow properties are observed. These include several density samples per layer, a detailed stratigraphic description, temperature, liquid water content if present, and preliminary crystal description, noting disaggregated appearance and *in situ* orientation. From this information representative domains are identified for sampling. Blocks of 700 ml or more are carefully cut from the pit wall and packed in containers in an ice chest with snow from the same layers. They are then transported to a cold laboratory, usually within a few hours of sampling. There subsamples are cut from each field sample for section plane preparation and for photography in a disaggregated state (Figure 1a). We prepare orthogonal sections for samples with suspected anisotropy.

The preparation of section planes in snow closely follows the recommendations of Perla [1982] and Perla and Dozier [1984]. A sample of snow is embedded in a supercooled organic liquid that is water-insoluble. Based on the extensive testing done by Perla [1982], we use dimethylpthalate at −5°C. The pore filler is dyed dark blue (oil blue N) to enhance the contrast with the ice grains. Freezing is started with a few grains of dry ice, sprinkled around the corners of the container. The section is then frozen rapidly at (−20°C) or colder.

Once frozen, the original orientation of the sample in the snowpack is marked, and the sample is roughly cut to a block about 3×3×5 cm. The block faces are then

planed with a microtome and left for about 10 min before further treatment. The ice grains have a much higher vapor pressure than the pore filler and differentially sublimate, particularly at the ice-pore boundary. The section surfaces are then polished with a find carbon fingerprint powder and high quality lens paper. With a delicate touch the ice grains are left outlined with the powder and the pore filler is smooth and shiny (Figure 1b).

Snow samples with especially fine structure may be difficult to plane and polish without plucking some ice fragments from the surface. In fine snow the ice grains can be allowed to sublimate more completely after initial planing, then planed again a few micrometers deeper. Polishing with lens papers and carbon powder will now fill the cavities left by the grains. The effects of evaporation of the pore filler can be tested by comparing the volume fractions of the object phase, ice, calculated from sections prepared by the two procedures.

3. Measurements from Sections

High contrast photographs are taken with a photomacroscope using a variety of 35 mm films (e.g. Kodak Ektachrome). A ring illuminator with fiber-optic light source provides specular reflection off the pore filler and minimizes sample heating. Generally the ice grains appear darker than the filler because they are more transparent, although occasionally bright reflections are observed from the interior of the ice grains. We get best results with illumination oriented parallel to the optical axis, although oblique illumination can also be used [W. Good, personal communication]. The images are scaled to actual lengths using photographs of a reference grid at various magnifications. Photographs are also taken of the grains in a disaggregated state.

The information contained in the section photographs is digitized and stored. At U.C. Santa Barbara we use a frame-grabber video digitizer, which is part of a Model 70F Image Computer from International Imaging Systems (I^2S). The digital image is then read to a VAX 11/780 from one of the memory channels on the image computer. Each section image is represented by 512×512 pixels with 8-bit brightness levels (0–255) and is classified as two phases: ice and pore space. At N.H.R.I. Canmore we use a Sony video photolab adapter HVT3000 and video camera

HVC2800. The digital image is read to an IBM PC. Each image has 240×250 pixels with 8-bit brightness levels.

Discrimination between ice and pore filler in the digitized image is not without problems. Misclassification cannot be avoided using a simple discrimination based on a guess of a brightness level that seems to best separate the histogram into ice and pore areas (Figure 2). Surface flaws, uneven illumination, and spurious reflections from the bottom of the ice crystals are confounding effects. We are currently investigating alternative methods of classifying the digital image into ice and pore filler categories, instead of just using a brightness discrimination level [Haralick and Shapiro, 1985].

Currently the digital date are processed with a sampling technique that results in five measurement parameters and their distributions, but the possibilities certainly have not been exhausted:

(1) Point density P_P, the number of pixels falling on ice particles divided by the total number of pixels.

(2) Intercept number density N_L, the number of ice-pore and pore-ice transitions divided by the number of pixels.

(3) Ice intercept lengths L_i, the distances between pore-ice and ice-pore transitions.

(4) Pore intercept lengths L_p, the distances between ice-pore and pore-ice transitions.

(5) Tangents to the ice-profile boundary T_i, designated as positive or negative depending on local curvature.

The parameter distributions (mean, variance, minimum, and maximum) per line and over all lines are calculated for each image except for the profile tangent sums. For each snow sample two section images are stored: one cut parallel to the snow stratigraphic planes and the other orthogonal to them. This allows testing the assumption that the snow grains are randomly oriented and shows the need for measuring several sections or not. If the variance in the parameters between the orthogonal sections is small, the two may be averaged.

4. Stereologic Relations

Weibel [1979] proposes two general models for deciding the measurements of most value for a particular study. The first considers structural parameters only. The object phase (ice in this study) may have any shape, can be interconnected, and can have many concavities. The second model assumes that the object phase can be adequately described as discrete particles and usually assumes that the particles are convex in shape. Structural parameters can be defined in both models, the difference lying in the difficulty with counting individual grains in the first model. The discrete particle model including a particle shape assumption is needed to measure mean diameter, length of the grains, number of grains per unit volume, and other grain parameters.

Some structure parameters calculated are: (1) volume density V_V, from which the snow density can be calculated, (2) surface density S_V, of which specific surface (surface to volume ratio) of ice phase is a subset, (3) mean curvature density K_V, or mean surface curvature, and (4) mean intercept length L_i, which is related to the mean free path through the ice phase. All these are ratio estimates of statistical parameters and therefore subject to the standard estimates of error [Weibel, 1979, p. 95, p. 137].

Volume density is equal to the point density:

$$V_V = P_P = \frac{P_i}{P_T} \tag{1}$$

P_i is the number of pixels falling on ice, and P_T is the total number of pixels. Snow density ρ_s is

$$\rho_s = \rho_i P_P \tag{2}$$

where $\rho_i = 917$ kg m^{-3} is the density of ice.

Surface density, or surface area per containing volume, is

$$S_V = 2 N_L = 2 \frac{N_i}{L_T} \tag{3}$$

where N_L is the grain boundary intercept density, N_i is the number of profile boundary intersections, and L_T is the length of the line scan. The surface area calculation may be dependent on the magnification used to make the section image, that

is, the microscopic resolution. This effect has been known to cartographers for a long time in a lower dimension [Mandelbrot, 1967, 1983] and has been shown in biological studies [Keller *et al.*, 1976]. Volume density remains stable while S_V estimates usually increase with magnification. The effect may also be influenced by the technique, etching *vs.* filling, used to highlight the ice grains against the pore filler background.

Mean surface curvature is determined from the net tangent count:

$$K_V = \pi T_i = \pi \frac{T_{net}}{A_T} \tag{4}$$

T_{net} is the net (positive or negative) tangent count, and A_T is the total area of the section image. The parameter requires that the test grid be regular and equally spaced in orthogonal directions.

Mean intercept length is obtained as a primary measurement from the sections. We can distinguish between mean free path length in ice and in the pores.

5. Application Example

One potential use of plane sections is the measurement of those physical parameters of snow that are important in interpreting its electromagnetic signature. In modeling the reflectance of snow to solar radiation or the emissivity of snow for thermal radiation, to use Mie scattering theory demands the assumption that the scattering properties of the irregularly shaped grains can be appropriately mimicked by some sort of "equivalent sphere" [Wiscombe and Warren, 1980; Dozier and Warren, 1982]. Some proposed equivalences are the sphere of equal volume, equal projected area, equal surface area, or equal volume/surface ratio.

From plane sections it is possible to directly measure these parameters. Thus one could use radiative measurements to choose the spherical radius or radius distribtion that best explains the electromagnetic properties, and then compare these data to the plane section parameters, with the definition of "equivalent" chosen from the candidates listed above.

In the table below we present data from sections made from a snow pit on Mammoth Mountain, California, on February 11, 1985. The pack consisted of 80 cm of new snow, primarily one day old dendrites and needles, above 120 cm of older

snow in various stages of metamorphism. Samples from 5–12cm depth and 39–54 cm depth had the following size properties.

depth (cm)	orientation of section	bulk density ($kg\,m^{-3}$)	digital density ($kg\,m^{-3}$)	volume/ surface ratio (mm)	equivalent sphere radius (mm)
5 – 12	horz	196	193	0.182	0.061
5 – 12	horz	196	174	0.176	0.059
5 – 12	vert	196	211	0.199	0.066
39 – 54	horz	170	196	0.172	0.057
39 – 54	horz	170	188	0.174	0.058
39 – 54	vert	170	163	0.169	0.056

We have not yet processed the correlative reflectance measurements, but the grain radii are consistent with snow albedo for new snow [Wiscombe and Warren, 1980].

References

Dozier, J., and S. G. Warren, 1982. Effect of viewing angle on the infrared brightness temperature of snow. *Water Resources Research.* Vol. 18, pp. 1424-1434.

Good, W., 1982. Structural investigations of snow and ice on core III from the drilling on Vernagtferner, Austria, in 1979. *Zeitschrift für Gletscherkunde und Glazialgeologie.* Vol. 18, pp. 53-64.

Gubler, H., 1978. Determination of the mean number of bonds per snow grain and of the dependence of the tensile strength of snow on stereological parameters. *Journal of Glaciology.* Vol. 29, pp. 329-341.

Haralick, R. M., and L. G. Shapiro, 1985. Image segmentation techniques. *Computer Vision, Graphics, and Image Processing.* Vol. 29, pp. 100-132.

Keeler, C. M., 1969. The growth of bonds and the increase of mechanical strength in a dry seasonal snowpack. *Journal of Glaciology.* Vol. 8, pp. 441-450.

Keller, H. J., H. P. Friedli, P. Gehr, M. Bachofen, and E. R. Weibel, 1976. The effects of resolution on estimating stereologic parameters. *Proceedings, Fourth International Congress for Stereology.* E. E. Underwood, R. de Wit, and G. A. Moore, editors, National Bureau of Standards Special Publication 431, pp. 409-414.

Kry, P. R., 1975. Quantitative stereological analysis of grain bonds in snow. *Journal of Glaciology*. Vol. 14, pp. 467-477.

Mandelbrot, B. B., 1967. How long is the coast of Britain? Statistical self-similarity and fractional dimension. *Science*. No. 155, p. 636.

Mandelbrot, B. B., 1983. *The Fractal Geometry of Nature*. W. H. Freeman, San Francisco, CA.

Perla, R., 1982. Preparation of section planes in snow specimens. *Journal of Glaciology*. Vol. 28, pp. 199-204.

Perla, R., in press. Snow in strong or weak temperature gradients. Part II: Section-plane analysis. *Cold Regions Science and Technology*.

Perla, R., and J. Dozier, 1984. Observations of snow structure. *Proceedings, International Snow Science Workshop*. Mountain Rescue, Aspen, CO, pp. 182-188.

Underwood, E. E., 1970. *Quantitative Stereology*. Addison-Wesley, Reading, MA.

Vallese, F., and J. A. Kong, 1981. Correlation function studies for snow and ice. *Journal of Applied Physics*. Vol. 52, pp. 4921-4925.

Weibel, E. R., 1979. *Stereological Methods*, Vol. 1: *Practical Methods for Biological Morphometry*. Academic Press, New York, NY.

Weibel, E. R., 1980. *Stereological Methods*, Vol. 2: *Theoretical Foundations*. Academic Press, New York, NY.

Wiscombe, W. J., and S. G. Warren, 1980. A model for the spectral albedo of snow, 1, Pure snow. *Journal of the Atmospheric Sciences*. Vol. 37, pp. 2712-2733.

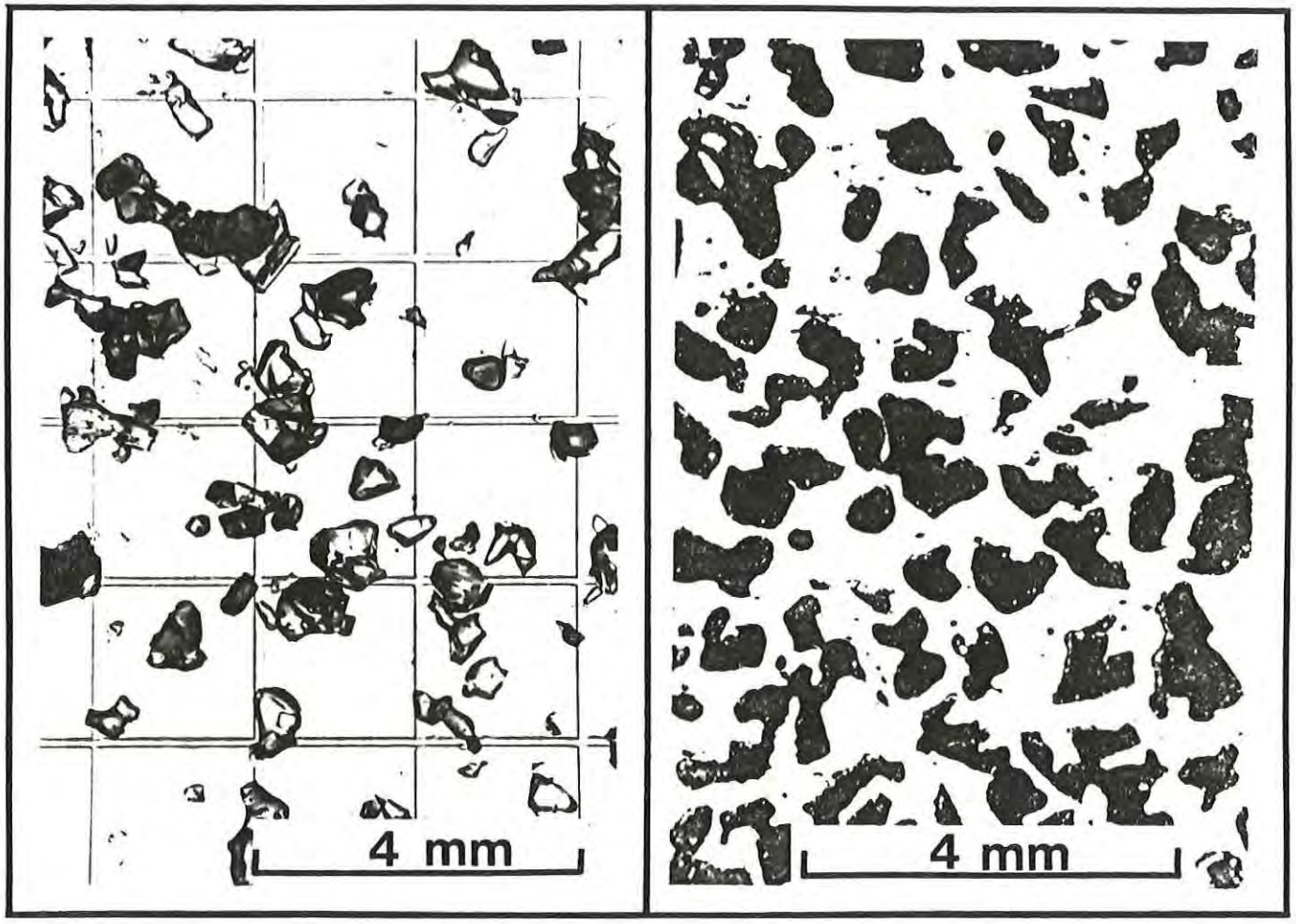

Figure 1a. Photomicrograph of disaggregated grains from a snow sample collected at middepth in a 1.5 m subalpine snowpit at Sunshine, Alberta. Sample density is 375 ± 5 kg/m^3. Crystals exhibit faceted and rounded morphology.

Figure 1b. Photomicrograph of a section-plane prepared from the sample described under Figure 1a. The section-plane was photographed using incident reflected light. Dark profiles represent ice. Some dark specks are probably not ice, and could be misclassified in an objective analysis. Conversely, some white specks may be misclassified as pore space.

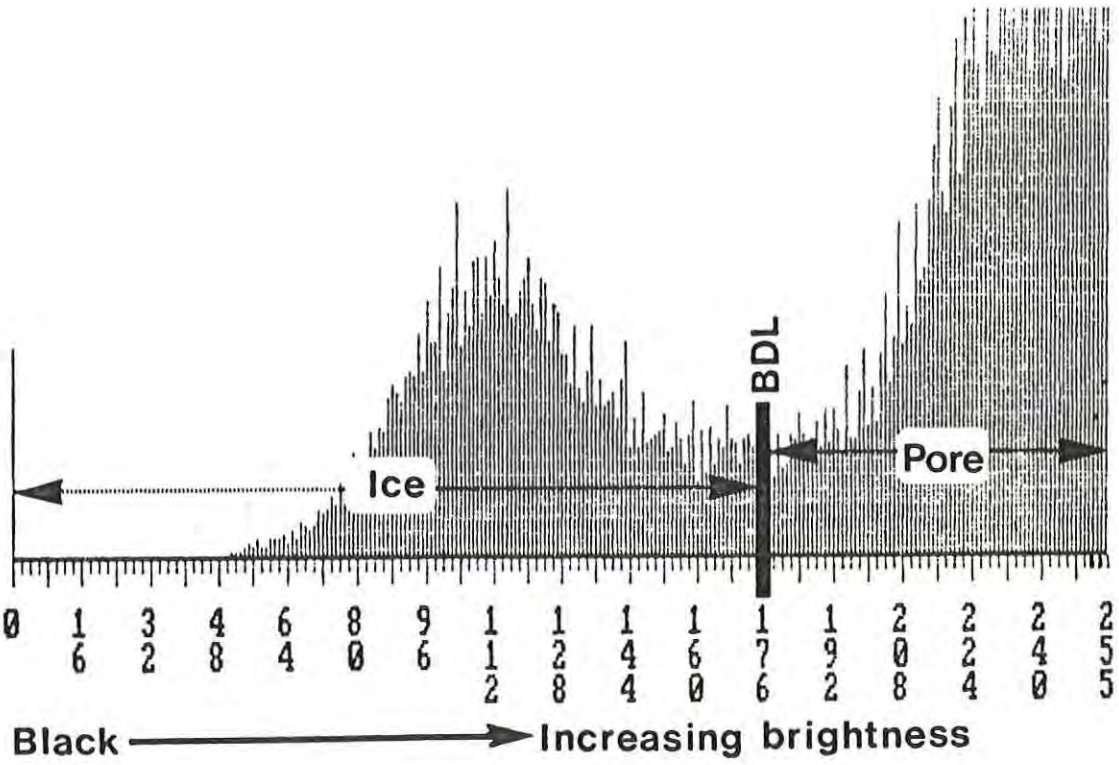

Figure 2. Brightness histogram from a video image of a section-plane photomicrograph. The relative number of pixel are shown at each brightness level from 0 to 225. Note that the histogram is truncated above about 225 because of anomalously high spikes at these higher brightness levels. A brightness discrimination level (BDL) is "guessed" to be at 176 to best separate the ice and pore profiles. This guess for BDL gave a reasonable replication of the qualitative shapes of the ice profile. However, the guess is not unique, and other BDL values in the approximate band 160 to 190 provide reasonable replication of ice shapes and measured sample density.